Desalination and Water Treatment
www.deswater.com
(2015) 1–13
doi: 10.1080/19443994.2014.1003103
Taylor & Francis
Taylor & Francis Group

Adsorption of caesium (Cs^+) from aqueous solution by porous titanosilicate xerogels

Olga Oleksiienko[a,b,*], Irina Levchuk[a], Maciej Sitarz[c], Svitlana Meleshevych[b], Volodymyr Strelko[b], Mika Sillanpää[a]

[a]*Laboratory of Green Chemistry, Lappeenranta University of Technology, Sammonkatu 12, Mikkeli 50130, Finland, Tel. +358 466297873; emails: ovalexis@gmail.com (O. Oleksiienko), Irina.Levchuk@lut.fi (I. Levchuk), Mika.Sillanpaa@lut.fi (M. Sillanpää)*
[b]*Institute of Sorption and Problems of Endoecology NAS of Ukraine, 13 General Naumov str., Kyiv 03164, Ukraine, emails: melesh@ispe.kiev.ua (S. Meleshevych), ispe@ispe.ldc.net (V. Strelko)*
[c]*Faculty of Materials Science and Ceramics, AGH University of Science and Technology, Al. Mickiewicza 30, Kraków 30059, Poland, email: msitarz@agh.edu.pl*

Received 12 September 2014; Accepted 21 December 2014

ABSTRACT

Two types of titanosilicate (TiSi) materials were synthesized by the sol–gel method using pure and technical precursors. All samples obtained were characterized using X-ray diffraction, FTIR in the mid-region and the low-temperature nitrogen adsorption/desorption technique. The synthesized xerogels were found to be amorphous with a developed porous structure. Solution pH, sample mass, initial Cs^+ concentration, competitive ions, contact time and temperature were studied for their influence on TiSi sorption ability. Both samples demonstrated a high capacity for caesium across a broad pH range of 2–12, and the adsorption isotherms were fitted to the Langmuir, Freundlich, Sips, Toth and Redlich–Peterson models, while the kinetic data were described using pseudo-first and pseudo-second models. All the TiSi samples were characterized by X-ray photoelectron spectroscopy and scanning electron microscopy with energy dispersive X-ray spectroscopy before and after the adsorption tests. Activated adsorption was proposed as a stage in the adsorption mechanism.

Keywords: Titanosilicates; Synthesis precursor; Xerogel pore structure; Adsorption capacity; Kinetic study

1. Introduction

Liquid radioactive waste (LRW) originates from many sources, including nuclear power plants, the mining industry, defence industry, nuclear medicine, nuclear research reactors and isotope laboratories [1,2]. The differences in the origins of LRW define the variety of its composition, which increase the requirements on decontamination materials and processes. There are many LRW treatment methods, including ion exchange, thermal evaporation, chemical precipitation, sedimentation and biological methods, and of those, ion exchange is currently the most commonly used method of LRW chemical processing [3–5]. Consequently, the synthesis of effective and stable ion exchange materials is a topical issue.

*Corresponding author.

It is well known that of the ion exchangers, ferrocyanides are the most selective for caesium, but they are efficient only in acidic medium [6–8]. In contrast, crystalline and poorly crystalline porous titanosilicates (TiSi) are effective and stable ion exchangers across a broad pH range [9–13]. Yet, both of these materials can be obtained in powder form only, which raises challenges for practical industrial applications. Recently, TiSi was synthesized by the sol–gel method [14,15], allowing to control the porosity, crystallinity, form and cost of the material. With the proposed method, it is possible to choose the fraction of sorbent particles (from 0.01 to 4 mm) after graining the xerogels. Sol–gel synthesis does not require cementation agents, which usually decrease the efficiency of sorption material. Therefore, the preparation time and the final cost of the product can also be reduced. Variation of the synthesis precursors broadened the field of sorbent application. For example, using an inexpensive (bulk grade) precursor yielded an ion exchanger for LRW mine and sea water. A pure precursor could achieve TiSi material for drinking water or blood plasma purification. This study seeks to investigate the influence of precursors on the sorption affinity and selectivity to Cs^+ of TiSi obtained by sol–gel synthesis using a chemically pure and technical solution of titanyl sulphate.

2. Experimental procedure

2.1. Chemicals

All chemicals used for the sorption tests (CsCl, NaCl, $NaHCO_3$, KCl, $CaCl_2$, H_2SO_4, HNO_3, HCl, NaOH, D-glucose) were of analytical grade (Sigma-Aldrich) and were used without further purification. Laboratory glassware washed with concentrated HCl or HNO_3 Milli-Q water (resistance 18.2 $M\Omega cm^{-1}$) was used for all experiments. Analytical grade solution of $TiCl_4$, technical solution of $TiOSO_4$ and technical solution of liquid glass ($Na_2O{\cdot}2.5SiO_2$) were bought from Ukrainian enterprises. Pure solution of $TiOSO_4$ was prepared by replacing Cl^- with SO_4^{2-} in $TiCl_4$.

2.2. Synthesis

TiSi samples were synthesized using the sol–gel method [14,15]. TiSi gels were obtained after a few minutes of intensive magnetic stirring of pure or technical $TiOSO_4$ solution (0.1 mmol), liquid glass (0.1 mmol) and NaOH (0.4 mmol) at room temperature. Thereafter, the prepared gels were hydrothermally treated (HTT) in steel autoclaves with Teflon beakers under autogenous pressure, and the synthesized TiSi gels were rinsed with water after HTT and dried at 80°C. Finally, the obtained xerogels were ground and sieved, and the fraction of 0.25–0.5 mm was used for the sorption tests.

2.3. Instrumentation

Specific surface area, pore size distribution and pore volume of TiSi xerogels were measured using a Quantachrome NOVA 2,200 surface area analyser. X-ray diffraction (XRD) patterns were obtained using DRON-4–07 (CuKα; 2θ = 5–80° step $\Delta 2\theta$ = 0.02°). FTIR spectra were recorded with a Bruker Vertex 70v spectrometer and collected in the mid (MIR)-region (4,000–100 cm^{-1}) after 128 scans at 4 cm^{-1} resolution. All samples were prepared by the standard KBr pellet method, and the microstructure of the produced materials was determined by scanning electron microscopy (SEM, Nova Nano SEM 200, FEI Company) with an attachment for the chemical analysis of specimens in micro-areas with energy dispersive X-ray spectroscopy. The experiment was carried out under low vacuum conditions in secondary electron mode. X-ray photoelectron spectroscopy (XPS) data were collected using a Thermo Fisher Scientific ESCALAB 250Xi Photoelectron Spectrometer. Measurements of pH were taken with a calibrated WTW 340i pH meter (WTW, Weilheim, Germany). A ST15 rotary shaker (CAT, M. Zipperer GmbH, Staufen, Germany) and IKA KS 4000i control shaker–incubator were used for sorption tests. To determine cation concentrations during the adsorption tests, an Agilent 7500ce inductively coupled plasma with mass detector was used.

2.4. Adsorption Experiments

Adsorption tests were conducted in batch technique using a shaker–incubator and rotary shaker with initial solutions prepared from solids. Aqueous solutions of caesium were used with different media: water, NaCl and Ringer–Locke's (RL) solution. All batch tests were performed in polypropylene tubes. Polypropylene syringe filters (size 0.45 μm) were used for sorbent separation. Adsorption capacity was studied as a function of pH, adsorbent mass, initial concentration, contact time, temperature, composition and concentration of background solution.

The influence of pH on the TiSi adsorption capacity (q) in Cs^+ solutions with water and 0.1 M NaCl media was evaluated, and experiments were conducted at a pH range of 2–12, with an initial Cs^+ concentration of 3.76 mmol L^{-1}. The solution volume to sorbent mass ratio (V:m) was 100, and the contact time was 24 h at ambient temperature (25 ± 2°C).

Effects of V:m ratio on the sorption capacity of TiSi were studied at V:m ratios ranging from 100 to 2,000 with an initial Cs^+ concentration of 3.76 mmol L^{-1}, water and 0.1 M NaCl as the solution media. pH was kept at 6.1 ± 0.2 and the contact time was 24 h at ambient temperature.

Influences of initial Cs^+ concentrations on q_{TiSi} were investigated in solutions with different media: water (pH = 6.1 ± 0.2); NaCl at concentrations of 0.05, 0.1 and 0.2 (pH = 6.1 ± 0.2); and RL solution (153.85 mmol L^{-1} of NaCl; 2.38 mmol L^{-1} of $NaHCO_3$; 2.68 mmol L^{-1} of KCl; 1.8 mmol L^{-1} of $CaCl_2$ and 5.55 mmol L^{-1} of D-glucose; pH = 8.07). Initial Cs^+ concentrations varied from 0.075 to 37.62 mmol L^{-1}, the V:m ratio was 100, and the contact time was 24 h at ambient temperature.

Effect of contact time (t) on q_{TiSi} was estimated using Cs^+ solutions with water, 0.1 M NaCl and RL media. Investigations were performed in a time range of 3–2,880 min at ambient temperature using an initial Cs^+ concentration of 3.76 mmol L^{-1} and a V:m ratio of 100.

Temperature effects on the Cs^+ solutions with 0.1 M NaCl and RL matrices were also investigated. Sorption tests were conducted at temperatures of 25, 40 and 60°C. The contact time was 3–180 min, the initial Cs^+ concentration was 3.76 mmol L^{-1}, and the V:m ratio was 100.

Adsorption capacity (q), distribution coefficient (K_d) and decontamination factor (DF) were calculated using the following equations:

$$\text{Adsorption capacity: } q = \Delta C \cdot \frac{V}{m} \tag{1}$$

where $\Delta C = C_o - C_t$, and C_o and C_t are the initial concentration and the concentration at time t of caesium in solution (mg L^{-1} or mmol L^{-1}), V is the aliquot volume (mL), and m is the mass of the adsorbent (g).

$$\text{Distribution coefficient: } K_d = \frac{\Delta C}{C_t} \cdot \frac{V}{m} \tag{2}$$

$$\text{Decontamination factor: } DF = (\Delta C \cdot 100\%)/C_0 \tag{3}$$

Experimental data were fitted to the Langmuir, Freundlich, Sips, Redlich–Peterson and Toth models, which are commonly used to describe liquid–solid systems [16] by the following equations:

$$\text{Langmuir: } q_e = \frac{q_m K_L C_e}{1 + K_L C_e} \tag{4}$$

where q_e is the adsorption capacity (mmol g^{-1}), C_e is the equilibrium concentration of the adsorbate (mmol L^{-1}), q_m is the maximum adsorption capacity of the adsorbent (mmol g^{-1}), and K_L is the Langmuir sorption equilibrium constant (L $mmol^{-1}$).

$$\text{Freundlich: } q_e = K_F C_e^{1/n_F} \tag{5}$$

where K_F ((mmol g^{-1})/(L $mmol^{-1})^{n}{}_F$) and n_F are the Freundlich adsorption constants.

$$\text{Sips: } q_e = \frac{q_m (K_S C_e)^{n_S}}{1 + (K_S C_e)^{n_S}} \tag{6}$$

where K_S is the affinity constant (L $mmol^{-1}$), and n_S is the Sips parameter for surface heterogeneity description.

$$\text{Redlich–Peterson: } q_e = \frac{q_m K_{RP} C_e}{1 + (K_{RP} C_e)^{n_{RP}}} \tag{7}$$

where K_{RP} and n_{RP} are the Redlich–Peterson constants.

$$\text{Toth: } q_e = \frac{q_m C_e}{(a_T + {C_e}^{m_T})^{\frac{1}{m_T}}} \tag{8}$$

where a_T is the adsorptive potential constant (mmol L^{-1}), and m_T is the Toth's heterogeneity factor.

The experimental kinetic data were fitted to the following models:

$$\text{nonlinear pseudo-first-order model: } q_t = q_e^{-k_1 t} \tag{9}$$

$$\text{linear pseudo-second-order model: } \frac{t}{q_t} = \frac{1}{k_2 q_e^2} + \frac{t}{q_e} \tag{10}$$

$$\text{and nonlinear pseudo-second-order model: } q_t = \frac{k_2 q_e^2 t}{1 + k_2 q_e t} \tag{11}$$

where q_t and q_e are the adsorption capacity (mmol g^{-1}) at time t and at equilibrium, respectively, while k_1 is the pseudo-first rate constant (L min^{-1}), k_2 is the pseudo-second rate constant (g $mmol^{-1}$ min^{-1}), and $k_2 {q_e}^2$ is the initial sorption rate.

To evaluate the correlation between the experimental data and the theoretical models, the coefficient of determination (R^2) was maximized with the MS Excel 2007 Solver Add-in:

$$R^2 = \frac{\sum(q_{e,exp} - \bar{q}_{e,exp})^2 - \sum(q_{e,exp} - q_{e,calc})^2}{\sum(q_{e,exp} - \bar{q}_{e,exp})^2} \quad (12)$$

where $q_{e,calc}$ is calculated from the isotherm equation equilibrium capacity, $q_{e,exp}$ is the experimentally obtained equilibrium capacity, and $\bar{q}_{e,exp}$ is the mean value of $q_{e,exp}$.

3. Results and discussion

3.1. Material characterization

The influence of the precursor on the adsorption affinity to Cs^+ was investigated for two types of TiSi xerogels: pure TiSi [TiSi(p)] obtained using a chemically pure solution of titanyl sulphate ($TiOSO_4$) and TiSi [TiSi(t)] synthesized using a technical solution of $TiOSO_4$. Both ion exchange materials were achieved in the amorphous phase, and therefore, no XRD patterns are shown here. FTIR studies were conducted in the mid-region (Fig. 1, with the analysed band positions and the suggested functional groups superimposed). As this figure shows, the bands most characteristic of bridged Si–O–Ti are present on both spectra at 971–956 cm^{-1}.

To investigate the pore structure of the xerogels, a low-temperature nitrogen adsorption/desorption technique was applied obtaining the following structural characteristics: TiSi(p) xerogel: Micro–mesopore structure, specific surface area (S_{BET})—270.3 $m^2 g^{-1}$, total pore volume (V_{total})—0.42 $cm^3 g^{-1}$, Dubinin–Radushkevich's micropore volume ($V_{DR\ micro}$)—0.1 $cm^3 g^{-1}$ and pore radius (R_{pore})—3.52 nm, $R_{micropore}$—2.5 nm; TiSi (t) xerogel: Micro–meso–macropore structure, S_{BET}—158.7 $m^2 g^{-1}$, V_{total}—0.47 $cm^3 g^{-1}$, $V_{DR\ micro}$—0.05 $cm^3 g^{-1}$, R_{pore}—8.4 nm, $R_{micropore}$—1.6 nm [17].

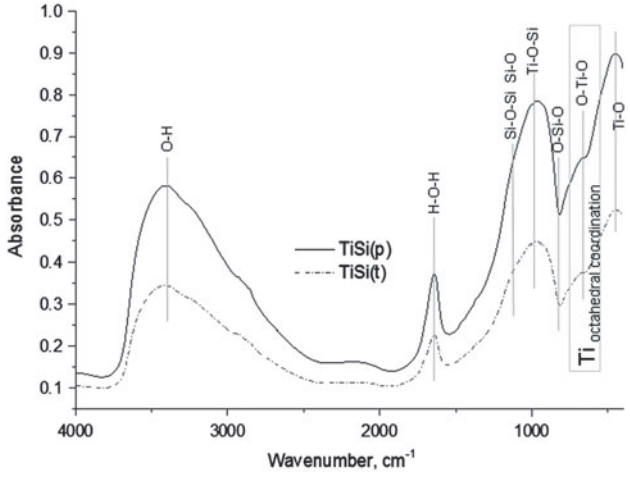

Fig. 1. FTIR spectrum of TiSi samples. Fraction size was 0.25–0.5 mm.

3.2. Sorption experiments

Adsorption studies were carried out with different background solutions in order to investigate the influence of competitive ions on the sorption capacity and selectivity of the obtained TiSi materials. Water was used as a medium for collecting the reference data. Of particular interest was the competition between Cs^+ and Na^+, since Na^+ is present at the highest concentration among the competing ions in real wastewaters and it is also present in drinking, sea and mine water [18–22]. To investigate this influence of the Cs^+/Na^+ competition and concentrations of competitive ions on the TiSi sorption capability, the NaCl background solution was used. With the RL solution, the ability of TiSi xerogels to remove Cs^+ in the presence of three competitive ions was examined: Na^+, K^+, Ca^{2+} [23,24]. Using the obtained data, the sorption ability and sorption mechanism of the synthesized materials in blood plasma, sea and drinking water can be predicted. As concentrations of these cations are substantially lower in drinking water than in sea water, it can be assumed that the TiSi sorption capability in drinking water ranges between the sorption capabilities for pure water and for the RL solution.

The first step of the current investigation was to determine the ability of the sol–gel synthesized TiSis to remove caesium from 3.76 mmol L^{-1} Cs^+ solution in water and 0.1 M NaCl background solution within a pH range from 2 to 12 (Fig. 2). It was found that in contrast to ferrocyanide powders, the obtained TiSi xerogels were able to remove Cs^+ across a broad pH range (2–12) with a high DF (DF ≥ 91% in water medium). It was shown that an increasing pH slightly reduces the DF for both materials in water: in 0.1 M NaCl, the reduction in DF for TiSi(p) was 14% and for TiSi(t) 10%. As has been shown by previous investigators, the cation adsorption, and cation exchange in particular, usually increases with pH [9,19,25–28]. Yet, the observed reverse effect could indicate a more complex Cs^+ removal mechanism than physisorption or ion exchange.

The selectivity of a sorption material is defined as a combination of physicochemical and stereochemical factors, such as ionic and hydrated radius, valency and electrostatic interaction, complexing ability and hydration energy, cation mobility and space requirement [25,26,29–31]. Consequently, sorption suppression could be attributed to an increased concentration of Na^+, since Na^+ has a higher complexing ability,

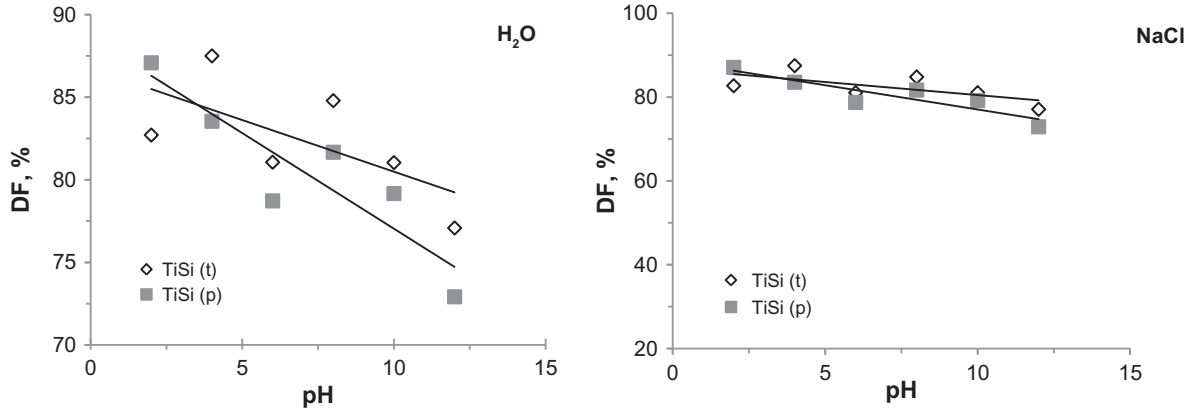

Fig. 2. Effect of pH on the DF of TiSi. Experimental conditions: pH from 2 to 12, initial Cs^+ concentration 3.76 mmol L^{-1}, water and 0.1 M NaCl media, *V*:*m* ratio 100, contact time 24 h, ambient temperature.

smaller hydrated and ionic radii and higher cation mobility than Cs^+. A similar suppression of H^+ to Cs^+ exchange was observed in the acidic pH region for the H-form of the powder TiSi [9,18]. Yet, such a low suppression at the evaluating concentration of competitive ions could also be related to the fact that Cs^+ has a lower (−263 kJ mol^{-1}) hydration energy than Na^+ (−405 kJ mol^{-1}), which may testify to the greater energy benefit of Cs uptake by TiSi xerogels [26,31,32]. The high DF and low influence of pH indicate the selectivity, chemical stability and capability of the synthesized materials for the effective removal of Cs cations from water and Na^+-containing solutions with a substantial initial Cs^+ concentration.

The second step of the present investigation was to determine the sufficient dose of the studied materials. In both studied background solutions, the adsorption ability decreased by less than 8% at a *V*:*m* ratio range from 100 to 2,000 for TiSi(t) and for both TiSi in water only (Fig. 3). It was found that the DF for both TiSis was around 90% at a sorbent concentration of 0.5 g L^{-1} and an initial Cs^+ concentration in water of 0.5 g L^{-1} (3.76 mmol L^{-1}). In a 0.1 M NaCl medium, the materials behaved differently: the DF of TiSi(p) decreased by 22% at a *V*:*m* ratio range from 100 to 2,000, which is 30% less than in water. This observation could be explained by the different porous structures of the obtained materials. Previous studies showed that sorption of Cs^+ and other alkali and alkaline earth cations occurs in micropores [10,11,33–35], and for TiSi with a rigid crystalline structure, less than 55% of ion exchange sites could be occupied by Cs^+ [19,33,36]. Poorly crystalline- or amorphous-structured TiSi with a developed porosity have better accessibility of Cs^+ ion-exchangeable sites [11,19]. An analogous situation was expected to occur with amorphous TiSi

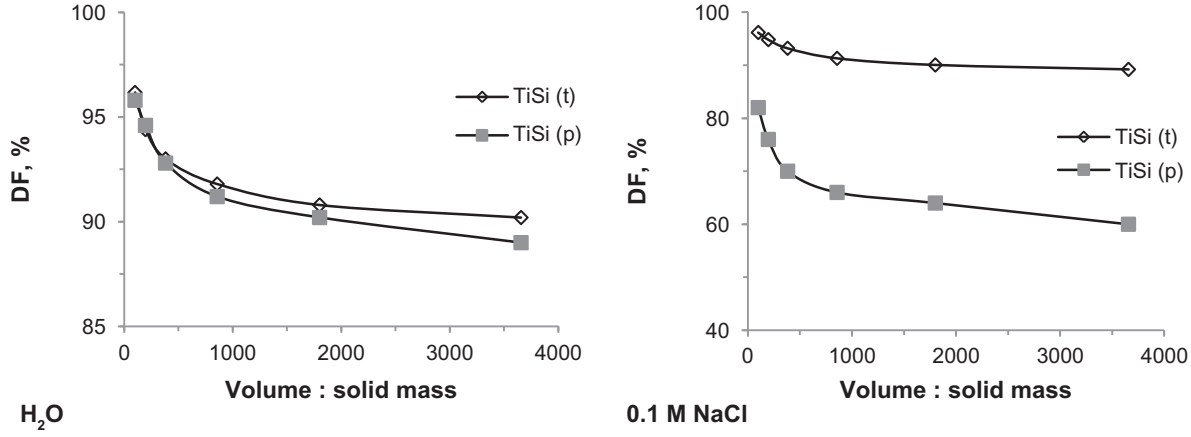

Fig. 3. Effect of the ratio between volume and sorbent mass on DF. Experimental conditions: initial Cs^+ concentrations 3.76 mmol L^{-1}, water and 0.1 M NaCl background solutions, ambient temperature.

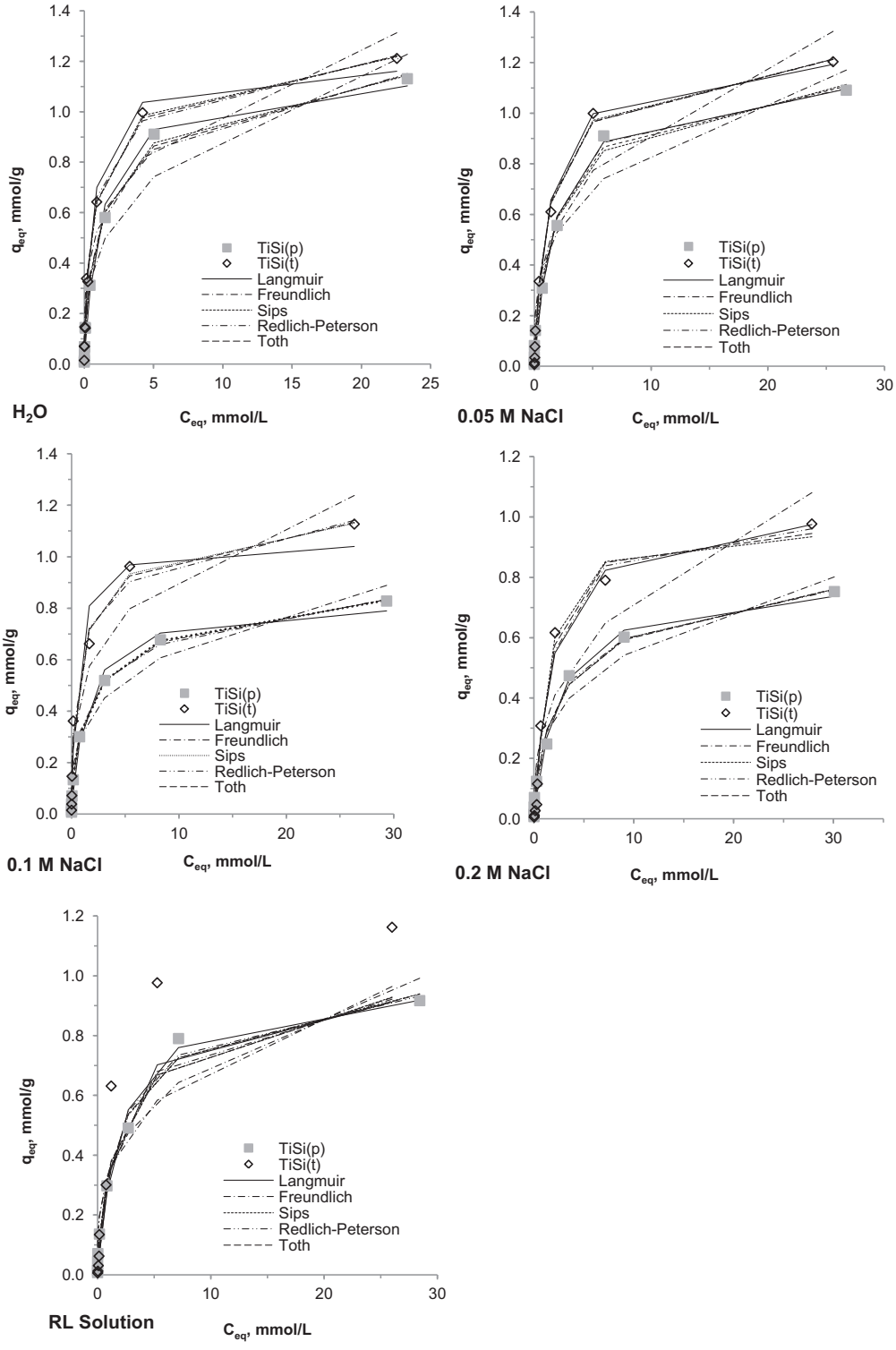

Fig. 4. Adsorption isotherms; experimental results: dots; results of modelling: lines. Experimental conditions: initial Cs^+ concentration range 0.075–37.62 mmol L^{-1}; *V*:*m* ratio 100; contact time 24 h; water; 0.05 M, 0.1 M and 0.2 M NaCl and RL solution media, ambient temperature.

xerogels. Therefore, it was suggested that the lower TiSi(t) micropore volume was compensated by a larger pore size, whereas large Cs^+ cations had fewer steric restrictions. Based on that assumption, it was decided to use a 10 g·L^{-1} dose of sorbent materials (V:m ratio 100) for further investigations, since at that dose a higher DF was observed.

The influence of the initial Cs^+ concentration on the TiSi adsorption ability was tested in water; 0.05, 0.1, 0.2 M NaCl; and RL solution at ambient temperature (Fig. 4). It was found that the adsorption isotherms for both xerogels synthesized from all studied media belong to the H2 shape according to the Giles classification [37,38]. This indicates the high affinity and selectivity to the adsorbate of the TiSi xerogels, and consequently, since the sorption isotherms were the same shape in different media, supposingly, there was a greater energy benefit in sorption with Cs^+ than with other competitive ions. It is important to note that the medium composition or concentration of competitive ions did not have any detectable influence up to an initial Cs^+ concentration of 3.76 mmol L^{-1}. An essential decrease in the TiSi capacity was observed at high initial Cs^+ concentrations (7.52–37.62 mmol L^{-1}). The results of the equilibrium adsorption capacity (q_{eq}) of the xerogels in different media show that q_{eq} was slightly lower at 0.05 M NaCl than in water (Table 1). In more complex and concentrated media, however, the adsorption capacity was 20–30% lower than in water, an effect that was similarly observed for powder TiSi [9,39]. It was found that TiSi(p) demonstrated $K_d(Cs^+)$ from 1×10^6 to 3×10^6 in all studied background solutions with a 0.075 mmol L^{-1} initial Cs^+ concentration, while TiSi(t) demonstrated $K_d(Cs^+)$ 8×10^6 in water with a 0.75 mmol L^{-1} initial Cs^+ concentration. The same order of K_d values was reported for crystalline powder TiSi analogues and ferrocyanides [7,19,28,36,40–42]. Thus, it can be concluded that (I) the TiSi(p) xerogel can be an efficient sorption material for drinking water and blood plasma and (II) the TiSi(t) xerogel can be used as an efficient sorbent for LRW, sea and mining water due to its higher q_{eq} in all tested media as well as wider pores, allowing the adsorption of cation pollutants both smaller and larger than Cs^+.

Kinetic tests were performed in water, 0.1 M NaCl and RL solution with an initial Cs^+ concentration of 3.76 mmol L^{-1}, the concentration at which the vertical part of the isotherms finished. Obviously, such a high initial concentration is not typical for real wastewaters, but in the vertical isotherm region at concentrations of 0.75 mmol L^{-1} and lower, kinetics is so fast that no substantial influence is observed [11,13]. For all experiments, the contact time ranged from 3 to 2,880 min at

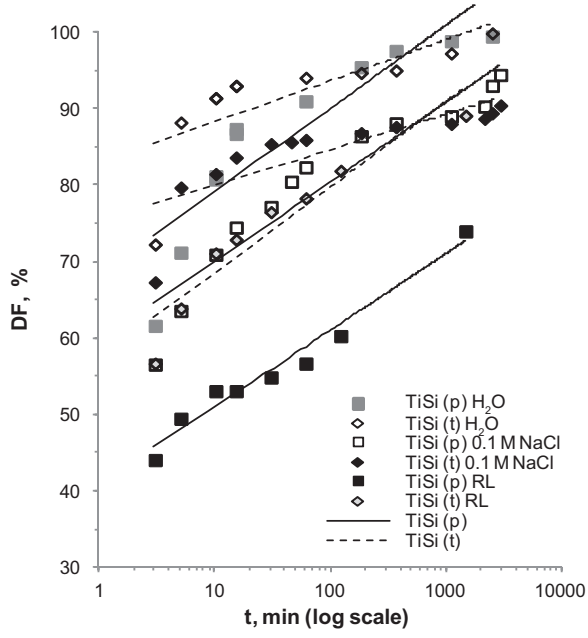

Fig. 5. Kinetics of Cs^+ sorption by TiSis. Experimental conditions: time range 3–2,880 min; initial Cs^+ concentration 3.76 mmol L^{-1}; V:m ratio 100; water and 0.1 M NaCl and RL background solutions, ambient temperature.

Table 1
The maximum adsorption capacity of Cs^+ by TiSi materials for different background solutions

	Background solution				
	q_{eq}, mmol/g				
		NaCl			
Sample type	H_2O	0.05 M	0.1 M	0.2 M	RL solution
TiSi(p)	1.13	1.091	0.83	0.75	0.92
TiSi(t)	1.21	1.203	1.13	0.98	1.16

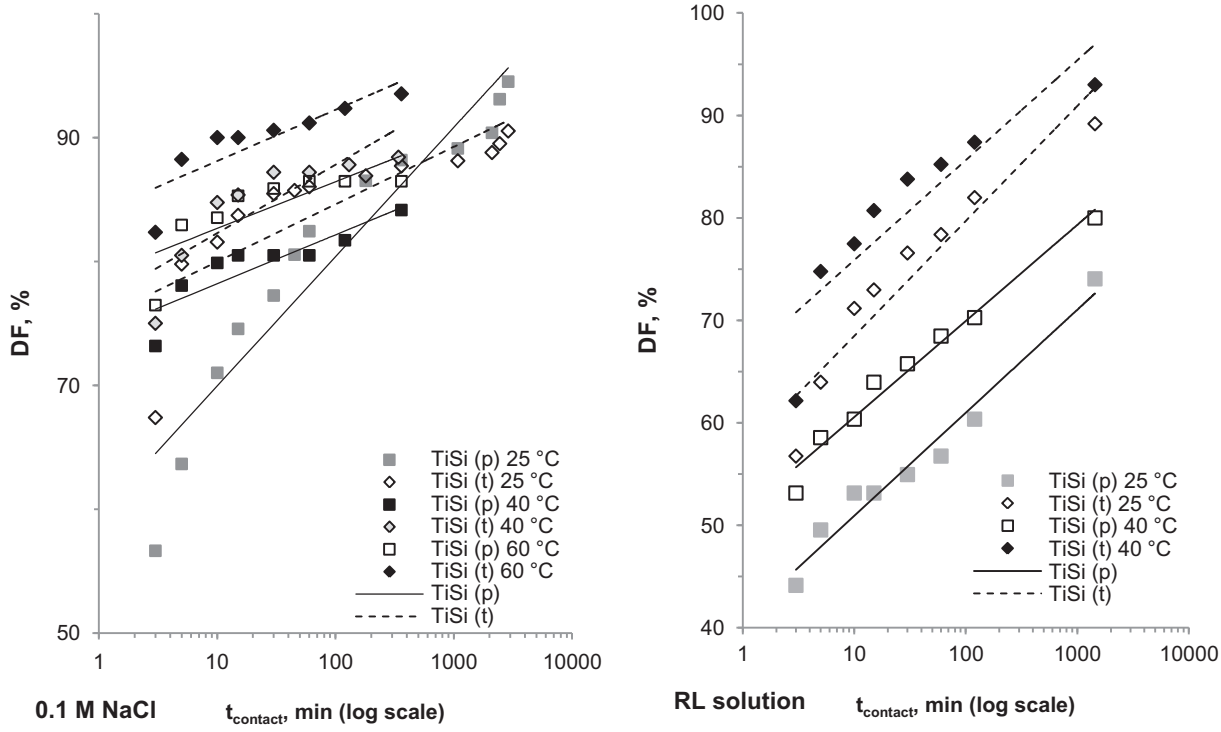

Fig. 6. Temperature effect on the kinetics of Cs^+ sorption. Experimental conditions: contact time 3–120 min; initial Cs^+ concentration 3.76 mmol L^{-1}; *V*:*m* ratio 100; temperature of adsorption 25, 40 and 60℃ for 0.1 M NaCl and RL media.

Table 2
Adsorption isotherm parameters obtained for studied TiSi

	TiSi(p)			TiSi(t)			TiSi(p)			TiSi(t)		
Model	q_{exp} mmol g^{-1}	q_{calc} mmol g^{-1}	R^2	q_{exp} mmol g^{-1}	q_{calc} mmol g^{-1}	R^2	q_{exp} mmol g^{-1}	q_{calc} mmol g^{-1}	R^2	q_{exp} mmol g^{-1}	q_{calc} mmol g^{-1}	R^2
Medium	H_2O						0.05 M NaCl					
Langmuir	1.131	1.102	0.985	1.211	1.161	0.979	1.091	1.096	0.987	1.203	1.193	0.996
Freundlich	1.131	1.228	0.958	1.211	1.313	0.943	1.091	1.170	0.965	1.203	1.324	0.929
Sips	1.131	1.144	0.998	1.211	1.218	0.991	1.091	1.114	0.990	1.203	1.213	0.998
Redlich–Peterson	1.131	1.151	0.993	1.211	1.223	0.988	1.091	1.098	0.987	1.203	1.213	0.997
Toth	1.131	1.148	0.996	1.211	1.22	0.990	1.091	1.107	0.988	1.203	1.215	0.998
Medium	0.1 M NaCl						0.2 M NaCl					
Langmuir	0.828	0.789	0.987	1.127	1.040	0.966	0.753	0.738	0.986	0.977	0.974	0.984
Freundlich	0.828	0.889	0.973	1.127	1.238	0.934	0.753	0.801	0.974	0.977	1.080	0.887
Sips	0.828	0.830	0.999	1.127	1.130	0.990	0.753	0.760	0.993	0.977	0.934	0.990
Redlich–Peterson	0.828	0.836	0.997	1.127	1.142	0.991	0.753	0.758	0.989	0.977	0.985	0.985
Toth	0.828	0.833	0.998	1.127	1.133	0.991	0.753	0.761	0.991	0.977	0.945	0.987
Medium	Ringer–Locke's solution											
Langmuir	0.917	0.918	0.985	1.162	0.912	0.979						
Freundlich	0.917	0.992	0.964	1.162	0.964	0.970						
Sips	0.917	0.940	0.990	1.162	0.929	0.978						
Redlich–Peterson	0.917	0.932	0.985	1.162	0.921	0.979						
Toth	0.917	0.938	0.988	1.162	0.927	0.979						

ambient temperature (Fig. 5), where both TiSi samples were able to remove Cs^+ rapidly and effectively. The difference in the kinetic rates for the obtained materials was attributed to their different porous structure. Fig. 5 illustrates that the TiSi(t) DF reached 91% after only 10 min of contact time, which is attributed to the wider pore distribution and larger average transport pore radius of the technical sample. Yet, pure TiSi showed a slower sorption kinetic and reached a DF of over 91% only after 1 h. In addition, the sorption rate of TiSi(p) was three times slower in a 0.1 M NaCl medium than in water and the sorption capacity of TiSi(t) was decreased in a 0.1 M NaCl medium with the kinetic curve having the same shape as for kinetic tests in water. It is noteworthy that the RL solution reduced the sorption rate and capacity of TiSi(t) only in the first 3 h, after which the DF was higher than that found in a NaCl background solution. In the RL medium, two additional competitive ions decreased the rate of TiSi(p) by two orders in the studied time period. As the TiSi(p) xerogel has wider micropores than TiSi(t), it was concluded that the transport pore radius is a rate-limiting parameter for TiSi xerogels, and presumably, the micropore volume will also play an essential role with increasing contact time.

Fig. 6 shows the effect of temperature on the kinetic of Cs^+ sorption by TiSi. Raising the

Table 3
Kinetic parameters for caesium sorption by TiSi for 0.1 M NaCl

		TiSi(p)				TiSi(t)			
Model	t ℃	q_{exp} mg g^{-1}	q_{calc} mg g^{-1}	k	R^2	q_{exp} mg g^{-1}	q_{calc} mg g^{-1}	k	R^2
Nonlinear pseudo-first-order expression	25*	0.39	0.38	0.51	0.999	0.39	0.38	0.51	0.968
	25	0.37	0.34	0.48	0.794	0.35	0.33	0.29	0.793
	40	0.40	0.36	0.29	0.000	0.35	0.31	0.53	0.575
	60	0.48	0.45	0.46	0.883	0.39	0.39	0.40	0.930
Linear pseudo-second-order expression	25*	0.39	0.41	2.89×10^{-6}	0.988	0.39	0.39	9.34×10^{-7}	0.738
	25	0.37	0.37	1.73×10^{-6}	0.394	0.35	0.37	2.76×10^{-6}	0.315
	40	0.40	0.41	1.05×10^{-5}	0.425	0.35	0.35	1.76×10^{-5}	0.708
	60	0.48	0.49	0.93×10^{-6}	0.367	0.39	0.37	9.37×10^{-6}	0.184
Nonlinear pseudo-second-order expression	25*	0.39	0.38	0.01	0.999	0.39	0.38	0.03	1.000
	25	0.37	0.35	0.03	0.818	0.35	0.34	0.01	0.980
	40	0.40	0.39	0.02	0.962	0.35	0.32	0.03	0.786
	60	0.48	0.47	0.02	0.908	0.39	0.39	0.02	0.912

*Adsorption for H_2O.

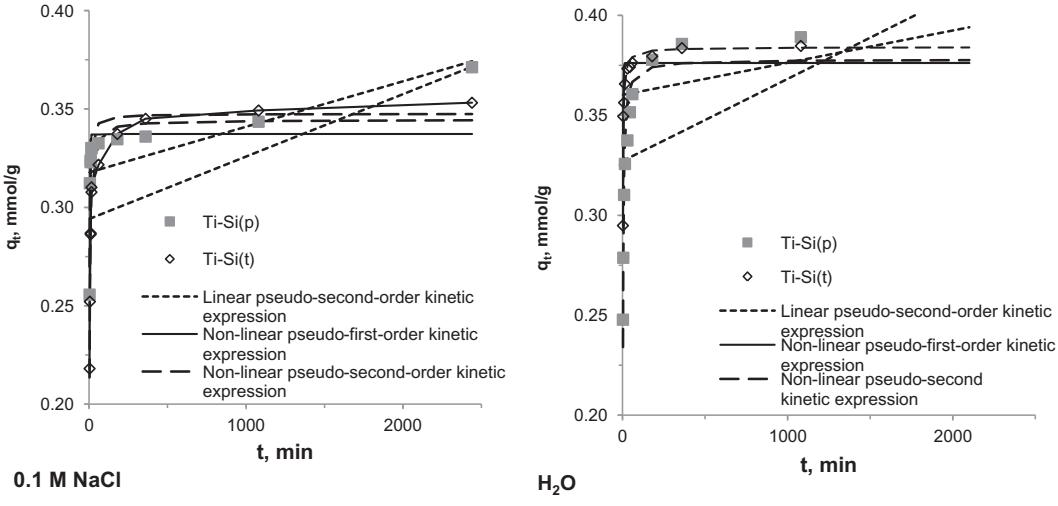

Fig. 7. Kinetic data of Cs^+ sorption fitted to theoretical models; experimental results: dots; results of modelling: lines.

temperature had a substantial impact on the TiSi(p) adsorption rate in the first 10 min. A temperature increase from 25 to 40˚C raises the DF by 20% in the first 3 min, whereas the DF after 10 min at 40˚C reached the same level as after 60 min at 25˚C. It was found that the Cs^+ uptake increased by 10% every 15–20˚C in 0.1 M NaCl and in RL solution for both tested materials. Following the literature, sorption processes based on physical phenomena such as ion exchange decrease with increasing temperature [7,43,44]. The increasing sorption rate could be attributed to the enhanced mobility of caesium ions or suggests that Cs^+ is removed by an activated sorption (when the elevated temperature raises the concentration of dehydrated Cs^+), or chemisorption mechanism [45–48].

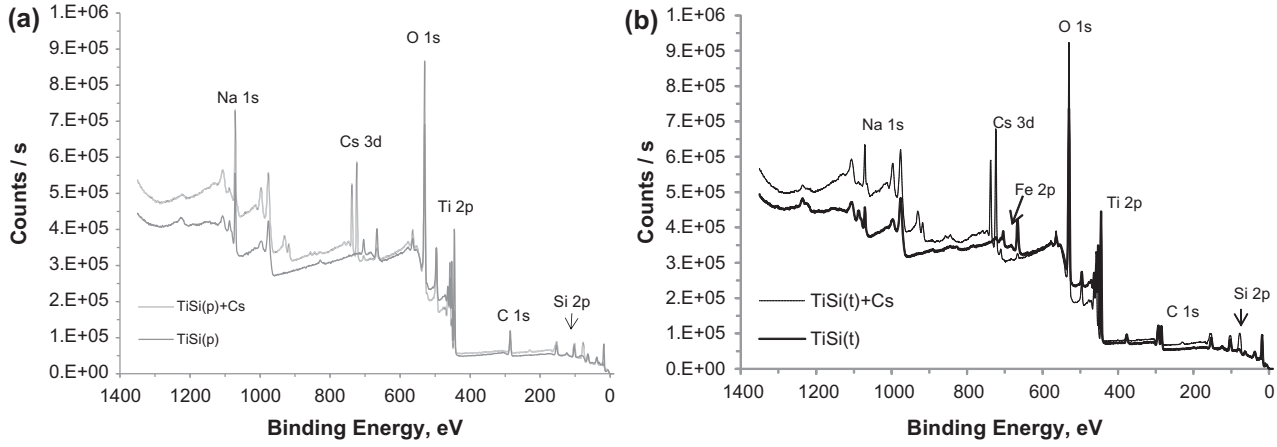

Fig. 8. XPS spectra of TiSi xerogels before and after the adsorption tests: (a) TiSi(p); (b) TiSi(t).

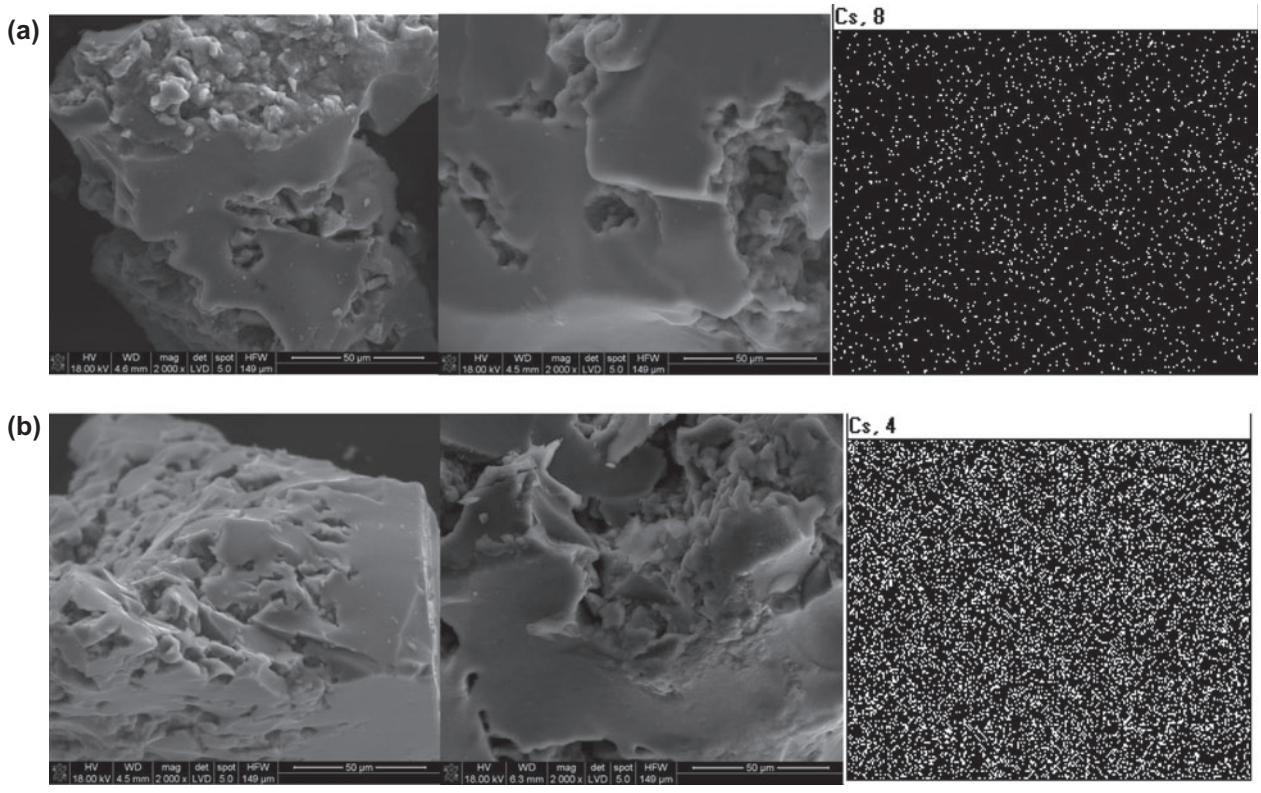

Fig. 9. SEM images of *a*-TiSi(p) and *b*-TiSi(t) xerogels before and after Cs^+ adsorption with mapping data for samples after the sorption tests.

In order to understand the character of the sorption process, the obtained isotherm adsorption data were fitted to theoretical models: the Langmuir, Freundlich, Sips, Redlich–Peterson and Toth models. Table 2 and Fig. 4 demonstrate that the adsorption isotherms of TiSi are better described by models that consider surface heterogeneity. While the Sips model describes TiSi(p) experimental data better than the other models in all matrices ($R^2 \geq 0.99$), the isotherms of TiSi(t) fits best to the Sips, Redlich–Peterson and Toth models ($R^2 \geq 0.98$). Fitting the adsorption kinetic experimental data to nonlinear pseudo-first-order, linear and nonlinear pseudo-second order-theoretical models showed that the nonlinear pseudosecond order model proved to be the most suitable model ($R^2 \geq 0.98$, Table 3 and Fig. 7). This pseudo-second-order model suggests chemisorption involving exchanging or sharing of electrons as a rate-limiting step [45–49]. Since the pH dependence for both TiSi was atypical for a physisorption process and the sorption rate rose with elevated temperature and kinetic data followed pseudo-second-order models, activated sorption or chemisorption mechanisms were considered.

XRD, XPS and SEM data were collected for both TiSi materials before and after the adsorption tests, and the XPS spectra show the presence of caesium on both studied materials (Fig. 8). An XRD is not shown since the samples stayed amorphous and no crystalline heterophase appeared. Fig. 9 illustrates that the sample microstructure did not change during the sorption test and no heterophase was observed. Mapping data demonstrated the homogeneous distribution of Cs across the studied surfaces.

Activated sorption was thus considered as the mechanism of the Cs^+ uptake. Activated adsorption allows to ascribe the obtained temperature dependence to the endothermic nature of the cation dehydrating process. Earlier investigations showed that cations exchanged in dehydrated form for TiSis and for sodium titanate [30,31]. An activated adsorption mechanism implies the presence in the TiSi xerogel structure of micropores whose radius is very similar to that of dehydrated Cs^+ ions. Fine fixation of Cs^+ in channels with an inner radius of similar size to Cs^+ ionic radii was reported for crystalline TiSis with a developed framework structure [11,19].

4. Conclusions

As could been shown, substituting a pure precursor with a technical one not only reduces the final cost of the material but promotes the formation of xerogels with a more developed mesoporous structure. TiSis obtained by sol–gel synthesis from pure and technical precursors proved highly efficient sorbent materials for caesium uptake from aqueous solutions across a broad pH range. The adsorption affinity of TiSi(t) was not substantially higher than that of the material obtained from a pure precursor. Studies of the influence of background solution showed that neither medium composition nor competitive ion concentration had a detectable impact on sorption ability. Selectivity was observed up to an initial Cs^+ concentration of 3.76 mmol L^{-1}. At ambient temperature, the process rate is relatively rapid with slight increases at higher temperatures, and the sorption process for pure and technical TiSi with water and 0.1 M NaCl media follows the pseudo-second-order kinetic model. It is proposed that the Cs^+ uptake occurs via an activated sorption mechanism. Furthermore, it is assumed that the TiSi xerogel structure contained micropores with radii very similar in size to Cs^+ ion radii. In addition, the obtained data proved that synthesized TiSi(p) xerogels can be effective sorption materials for drinking water as well as blood plasma, whereas the TiSi(t) xerogel could be an efficient sorbent for LRW, sea and mine water, due to its high adsorption capacity in all tested media and wide pore size distribution for the adsorption of cationic pollutants both smaller and larger than Cs^+.

Acknowledgements

The authors thank Elisa Alasuvanto for her assistance with the sorption experiments. We are also grateful to Yurij M. Kylivnyk and Valerij I. Yakovlev for assisting with the precursor preparation and for our fruitful discussions. Furthermore, we thank Mukola M. Tsyba for supporting the porous investigations and Kate Sotejeff–Wilson for our fruitful discussions and language support. We greatly acknowledge Prof. Christian Wolkersdorfer for fruitful discussions, language and technical support.

References

[1] R.D. Ambashta, M.E.T. Sillanpää, Membrane purification in radioactive waste management: A short review, J. Environ. Radioact. 105 (2012) 76–84.
[2] UNSCEAR (United Nations Scientific Committee on the Effects of Atomic Radiation), Sources and Effects of Ionizing Radiation, United Nations Scientific Committee on the Effects of Atomic Radiation, UNSCEAR, New York, NY, 2011.
[3] IAEA, Improvements of Radioactive Waste Management at WWER Nuclear Power Plants, IAEA, TECDOC-1492, Vienna, 2006.

[4] IAEA, Nuclear Safety Review, IAEA, GC(57)/INF/3, Vienna, 2013, 1.
[5] R. Harjula, J. Lehto, A. Paajanen, E. Tusa, P. Yarnell, Use inorganic ion exchange materials as precoat filters for nuclear waste effluent treatment, React. Funct. Polym. 60 (2004) 85–95.
[6] IAEA, Technologies for Remediation of Radioactively Contaminated Sites, Technologies for Remediation of Radioactively Contaminated Sites, IAEA, TECDOC-1086, Vienna, 1999.
[7] F. Han, G. Zhang, P. Gu, Adsorption kinetics and equilibrium modeling of cesium on copper ferrocyanide, J. Radioanal. Nucl. Chem. 295 (2013) 369–377.
[8] T.D. Clarke, C.M. Wai, Selective removal of cesium from acid solutions with immobilized copper ferrocyanide, J. Anal. Chem. 70 (1998) 3708–3711.
[9] T. Möller, R. Harjula, J. Lehto, Ion exchange of 85Sr, 134Cs and 57Co in sodium titanosilicate and the effect of crystallinity on selectivity, Sep. Purif. Technol. 28 (2002) 13–23.
[10] A. Clearfield, D.G. Medvedev, S. Kerlegon, T. Bosser, J.D. Burns, J. Milton, Rates of exchange of Cs^+ and Sr^{2+} for poorly crystalline sodium titanium silicate (CST) in nuclear waste systems, Solvent Extr. Ion Exch. 30 (2012) 229–243.
[11] O.V. Oleksiienko, S.I. Meleshevych, V.V. Strelko, O.I. V'yunov, O.K. Matkovsky, V.G. Milgrandt, M.M. Tsyba, V.A. Kanibolotsky, Effect of hydrothermal treatment on the formation of the porous structure titanosilicates, Prob. Chem. Chem. Technol. 2 (2013) 101–105.
[12] K. Popa, C.C. Pavel, Radioactive wastewaters purification using titanosilicates materials: State of the art and perspectives, Desalination 293 (2012) 78–86.
[13] G. Lujaniene, S. Meleshevych, V. Kanibolotskyy, J. Sapolaite, V. Strelko, V. Remeikis, O. Oleksiienko, K. Ribokaite, T. Sciglo, Application of inorganic sorbents for removal of Cs, Sr, Pu and Am from contaminated solutions, J. Radioanal. Nucl. Chem. 282 (2009) 787–791.
[14] V.G. Kalenchuk, S.V. Meleshevych, V.A. Kanibolotsky, V.V. Strelko, O.V. Oleksiienko, N.M. Patryliak, A method for producing titanosilicate ionexchanger, UA patent 48457 (2010).
[15] V.V. Strelko, S.V. Meleshevych, V.A. Kanibolotsky, O.V. Oleksiienko, A method for producing titanosilicate ionexchanger, UA patent 66489 (2012).
[16] K.Y. Foo, B.H. Hameed, Insights into the modeling of adsorption isotherm systems, Chem. Eng. J. 156 (2010) 2–10.
[17] O. Oleksiienko, I. Levchuk, M. Sitarz, S. Meleshevych, V. Strelko, M. Sillanpää, Removal of strontium (Sr^{2+}) from aqueous solutions with titanosilicates obtained by the sol–gel method, J. Colloid Interface Sci. 438 (2015) 159–168.
[18] A.I. Bortun, L.N. Bortun, A. Clearfield, Evaluation of synthetic inorganic ion exchangers for cesium and strontium removal from contaminated groundwater and wastewater, Solvent Extr. Ion Exch. 15 (1997) 909–929.
[19] E.A. Behrens, A. Clearfield, Titanium silicates, $M_3HTi_4O_4(SiO_4)_3{\cdot}4H_2O$ ($M = Na^+$, K^+), with three-dimensional tunnel structures for the selective removal of strontium and cesium from wastewater solutions, Microporous Mater. 11 (1997) 65–75.
[20] A. Tripathi, D.G. Medvedev, A. Clearfield, The crystal structures of strontium exchanged sodium titanosilicates in relation to selectivity for nuclear waste treatment, J. Solid State Chem. 178 (2005) 253–261.
[21] F.J. Maringer, J. Šuráň, P. Kovář, B. Chauvenet, V. Peyres, E. García-Toraño, M.L. Cozzella, P. De Felice, B. Vodenik, M. Hult, U. Rosengård, M. Merimaa, L. Szücs, C. Jeffery, J.C.J. Dean, Z. Tymiński, D. Arnold, R. Hinca, G. Mirescu, Radioactive waste management: Review on clearance levels and acceptance criteria legislation, requirements and standards, Appl. Radiat. Isot. 81 (2013) 255–260.
[22] C. Wolkersdorfer, Water Management at Abandoned Flooded Underground Mines—Fundamentals, Tracer Tests, Modelling, Water Treatment, Springer, Heidelberg, 2008.
[23] J.P. Steel, The treatment of certain mental diseases by Ringer–Locke solution, Br. Med. J. 2 (1927) 1177–1178.
[24] W.R. Amberson, J. Flexner, F.R. Steggerda, A.G. Mulder, M.J. Tendler, D.S. Pankratz, E.P. Laug, On the use of Ringer–Locke solutions containing hemoglobin as a substitute for normal blood in mammals, J. Cell. Comp. Physiol. 5 (1934) 359–382.
[25] A. Dyer, J. Newton, L. O'Brien, S. Owens, Studies on a synthetic sitinakite-type silicotitanate cation exchanger: Part 1: Measurement of cation exchange diffusion coefficients, Microporous Mesoporous Mater. 117 (2009) 304–308.
[26] A. Dyer, J. Newton, L. O'Brien, S. Owens, Studies on a synthetic sitinakite-type silicotitanate cation exchanger. Part 2. Effect of alkaline earth and alkali metals on the uptake of Cs and Sr radioisotopes, Microporous Mesoporous Mater. 120 (2009) 272–277.
[27] N. Bolong, A.F. Ismail, M.R. Salim, T. Matsuura, A review of the effects of emerging contaminants in wastewater and options for their removal, Desalination 239 (2009) 229–246.
[28] V.V. Milyutin, S.V. Mikheev, V.M. Gelis, E.A. Kozlitin, Sorption of cesium on ferrocyanide sorbents from highly saline solutions, Radiochemistry 51 (2009) 298–300.
[29] I.M. El-Naggar, E.A. Mowafy, E.A. Abdel-Galil, Diffusion mechanism of certain fission products in the particles of silico(IV)titanate, Colloids Surf., A 307 (2007) 77–82.
[30] I.M. El-Naggar, E.A. Mowafy, I.M. Ali, H.F. Aly, Synthesis and sorption behaviour of some radioactive nuclides on sodium titanate as cation exchanger, Adsorption 8 (2002) 225–234.
[31] I.M. Ali, E.S. Zakaria, H.F. Aly, Highly effective removal of ^{22}Na, ^{134}Cs and ^{60}Co from aqueous solutions by titanosilicate: A radiotracer study, J. Radioanal. Nucl. Chem. 285 (2010) 483–489.
[32] J. Burgess, Metal ions in solutions, Ellis Horwood, Chichester, 1978.
[33] E.A. Behrens, D.M. Poojary, A. Clearfield, Syntheses, crystal structures, and ion-exchange properties of porous titanosilicates, $HM_3Ti_4O_4(SiO_4)3A\ 4H_2O$ ($M = H^+$, K^+, Cs^+), structural analogues of the mineral pharmacosiderite, Chem. Mater. 8 (1996) 1236–1244.
[34] P. Sylvester, E.A. Behrens, G.M. Graziano, A. Clearfield, An assessment of inorganic ion-exchange materials for the removal of strontium from simulated hanford tank wastes, Sep. Sci. Technol. 34 (1999) 1981–1992.

[35] A. Clearfield, Inorganic ion exchangers, past, present, and future, Solvent Extr. Ion Exch. 18 (2000) 655–678.
[36] D.M. Poojary, R.A. Cahill, A. Clearfield, Synthesis, crystal structures, and ion-exchange properties of a novel porous titanosilicate, Chem. Mater. 6 (1994) 2364–2368.
[37] C.H. Giles, R.B. Mackay, Adsorption of cationic (basic) dyes by fixed yeast cells, J. Bacteriol. 89 (1965) 390–397.
[38] C.H. Giles, T.H. MacEwan, S.N. Nakhwa, D. Smith, 786. Studies in adsorption. Part XI. A system of classification of solution adsorption isotherms, and its use in diagnosis of adsorption mechanisms and in measurement of specific surface areas of solids, J. Chem. Soc. (1960) 3973–3993.
[39] J. Lehto, R. Harjula, Selective separation of radionuclides from nuclear waste solutions with inorganic ion exchangers, Radiochim. Acta 86 (1999) 65–70.
[40] D. Huys, L.H. Baetslé, A new series of synthetic acid stable mineral ion exchangers—I. Ferrocyanide-molybdate (FeMo), J. Inorg. Nucl. Chem. 26 (1964) 1329–1331.
[41] A. Clearfield, L.N. Bortun, A.I. Bortun, Alkali metal ion exchange by the framework titanium silicate $M_2Ti_2O_3SiO_4{\cdot}nH_2O$ (M=H, Na), React. Funct. Polym. 43 (2000) 85–95.
[42] A. Clearfield, Structure and ion exchange properties of tunnel type titanium silicates, Solid State Sci. 3 (2001) 103–112.
[43] L.E. Katz, L.J. Criscenti, C. Chen, J.P. Larentzos, H.M. Liljestrand, Temperature effects on alkaline earth metal ions adsorption on gibbsite: Approaches from macroscopic sorption experiments and molecular dynamics simulations, J. Colloid Interface Sci. 399 (2013) 68–76.
[44] W. Zuo, P. Han, Y. Li, X. Liu, X. He, R. Han, Equilibrium, kinetic and mechanism study for adsorption of neutral red onto rise husk, Desalin. Water Treat. 12 (2009) 210–218.
[45] Y.S. Ho, J.F. Porter, G. McKay, Equilibrium isotherm studies for the sorption of divalent metal ions onto peat: Copper, nickel and lead single component systems, Water Air Soil Pollut. 141 (2002) 1–33.
[46] Y.S. Ho, G. McKay, Pseudo-second order model for sorption processes, Process Biochem. 34 (1999) 451–465.
[47] T. Wolkenstein, Electronic processes on semiconductor surfaces during chemisorption, Bureau, New York, NY, 1991.
[48] T. Wolkenstein, Activated adsorption on semiconductors, Uspehi Fizicheskih Nauk. 2 (1953) 253–270.
[49] W.G. Pollard, Use of surface states to explain activated adsorption, Phys. Rev. 56 (1939) 324–336.